Geophysical Prospecting

EAGE EUROPEAN ASSOCIATION OF GEOSCIENTISTS & ENGINEERS

Geophysical Prospecting, 2011, **59**, 593–608 doi: 10.1111/j.1365-2478.2010.00943.x

Detection of multiple fracture sets using observations of shear-wave splitting in microseismic data

James P. Verdon* and J.-Michael Kendall

Department of Earth Sciences, University of Bristol, Bristol, BS8 1RJ, UK

Received July 2010, revision accepted November 2010

ABSTRACT

The hydrocarbon industry is moving increasingly towards tight sandstone and shale gas resources – reservoirs that require fractures to be produced economically. Therefore, techniques that can identify sets of aligned fractures are becoming more important. Fracture identification is also important in the areas of coal bed methane production, carbon capture and storage (CCS), geothermal energy, nuclear waste storage and mining. In all these settings, stress and pore pressure changes induced by engineering activity can generate or reactivate faults and fractures. P- and S-waves are emitted by such microseismic events, which can be recorded on downhole geophones. The presence of aligned fracture sets generates seismic anisotropy, which can be identified by measuring the splitting of the S-waves emitted by microseismic events. The raypaths of the S-waves will have an arbitrary orientation, controlled by the event and geophone locations, meaning that the anisotropy system may only be partly illuminated by the available arrivals. Therefore to reliably interpret such splitting measurements it is necessary to construct models that compare splitting observations with modelled values, allowing the best fitting rock physics parameters to be determined. Commonly, splitting measurements are inverted for one fracture set and rock fabrics with a vertical axis of symmetry. In this paper we address the challenge of identifying multiple aligned fracture sets using splitting measured on microseismic events.

We analyse data from the Weyburn CCS-EOR reservoir, which is known to have multiple fracture sets, and from a hydraulic fracture stimulation, where it is believed that only one set is present. We make splitting measurements on microseismic data recorded on downhole geophone arrays. Our inversion technique successfully discriminates between the single and multiple fracture cases and in all cases accurately identifies the strikes of fracture sets previously imaged using independent methods (borehole image logs, core samples, microseismic event locations). We also generate a synthetic example to highlight the pitfalls that can be encountered if it is assumed that only one fracture set is present when splitting data are interpreted, when in fact more than one fracture set is contributing to the anisotropy.

Key words: Fractures, Microseismic.

INTRODUCTION

Aligned fractures within a reservoir often play an important role in enhancing hydrocarbon production by providing pathways for fluid flow. Therefore, the ability to detect such

*E-mail: gljpv@bris.ac.uk

fractures is important for maximizing hydrocarbon production. The industry is moving increasingly towards more unconventional hydrocarbon resources such as tight gas, shale gas, and coalbed methane. Such reservoirs need fractures, either naturally occurring or induced by hydraulic fracture stimulation, in order to be produced economically. Therefore a growing need exists to develop techniques that can robustly identify fractures in situ. By identifying naturally occurring fractures, it is possible to target 'sweet-spots' with higher amounts of fracturing that produce at faster than expected rates. Similarly it is important to characterize the extent of fractures produced by hydraulic stimulation. The ability to detect and characterize fractures is also important to guarantee the caprock integrity of carbon dioxide storage projects, to maximize the efficiency of geothermal energy projects, to ensure safe underground storage of nuclear waste and to ensure safe excavation in mining operations.

A number of methods exist to identify and characterize fractures. One of the most effective in identifying aligned fracture sets, across a wider area than the point data sampling provided by boreholes, is to use seismic methods. Aligned fractures render a rock seismically anisotropic, meaning that the velocities of seismic waves travelling through the rock will depend on their direction of propagation and also their polarization. Seismic anisotropy manifests itself in a number of seismic observations, such as azimuthal variation in reflection amplitudes (e.g., Hall and Kendall 2000) and interval normal moveout (NMO) velocities (e.g., Bakulin, Grechka and Tsvankin 2000) in conventional reflection surveys.

Splitting of shear waves is another key indication of seismic anisotropy: when a shear wave travels through an anisotropic region it will be split into two orthogonally polarized waves, one of which will travel faster than the other. The polarisation of the fast wave (ψ), and the time lag (δt) between the arrivals of the fast and slow wave, can be measured on a 3-component geophone and characterizes the splitting along a raypath. Usually, δt is normalised by ray path length to give the percentage difference between fast and slow S-wave velocities, δV_S. To characterize the type of anisotropic symmetry system and its orientation and strength, either splitting measurements from a range of propagation directions, or other geophysical constraints, are required.

Shear wave splitting (SWS) is used as a matter of course in global seismological studies (e.g., Kendall *et al.* 2006) to identify such features as fractures (e.g., Crampin 1991; Boness and Zoback 2006), melt inclusion alignment (e.g., Blackman and Kendall 1997; Kendall *et al.* 2005), alignment of crystals caused by mantle flow (e.g., Blackman *et al.* 1993; Rümpker, Tommasi and Kendall 1999; Barruol and Hoffmann 1999) and the nature of the Earth's solid inner core (Wookey and Helffrich 2008). SWS has even been suggested as a tool for predicting the occurrence of earthquakes (Crampin, Gao and Peacock 2008). More recently, SWS measured on controlled-source surveys, both reflection and vertical seismic profiling (VSP), have become more common (e.g., Shuck, Davis and Benson 1996; Winterstein, De and Meadows 2001; Davis *et al.* 2007), although their use is still not widespread. Despite these successes, SWS measured on microseismic events is rarely used to detect seismic anisotropy in reservoir settings.

Hydraulic stimulation is often used to generate fractures around a well, improving production by providing high permeability flow pathways (e.g., Le Calvez *et al.* 2005). Fractures and faults can also be formed or reactivated by geomechanical deformation in and around a reservoir that is undergoing pore pressure alteration during hydrocarbon production (e.g., Angus *et al.* 2010) or fluid injection. Movement of faults and/or fractures generates P and S-wave seismic energy. Although analogous to earthquakes, in and around reservoirs event magnitudes are usually smaller, so they are referred to as microearthquakes or microseismic events. Downhole geophone arrays can be deployed to detect the seismic energy emitted with the aim of locating the microseismic event hypocenters and thereby imaging the fractures. However, because these events emit S-wave energy, which is recorded on 3-component geophones, they represent excellent shear-wave sources for identifying fractures using SWS as well. Because the recorded energy has usually travelled only through the reservoir and the overburden close to the reservoir (depending on array geometry of course), the anisotropic effects can be attributed solely to these rocks. There is no need to account for the anisotropy of all the rock between the surface and the reservoir interval, as with shear-wave splitting measured using 9-component reflection seismic surveys (e.g., Luo *et al.* 2005, 2007). However, interpretation of SWS measurements on induced microseismic events is made more complicated by the fact that recorded waves will have propagated at arbitrary angles through the subsurface. From both the rock physics theory and lab and field observations (e.g., Crampin and Peacock 2008), for a given anisotropic system, we know that ψ and δV_S are highly dependent on the direction of propagation. This is particularly true for anisotropy systems with lower degrees of symmetry.

As well as aligned fracture sets, seismic anisotropy can be generated by many types and length-scales of structure, such as the alignment of anisotropic minerals (Valcke *et al.* 2006; Kendall *et al.* 2007), the alignment of grain-scale

compliant pore spaces (e.g., Hall *et al.* 2008), which can be distorted by non-hydrostatic stress changes (e.g., Verdon *et al.* 2008). In oil reservoirs these features tend to align subhorizontally, creating an anisotropic system with a vertical axis of symmetry, termed vertical transverse isotropy (VTI). Aligned subvertical fractures in an isotropic background generate an anisotropic system with a horizontal axis of symmetry, termed horizontal transverse isotropy (HTI). When a VTI system is combined with an HTI fracture system, anisotropic systems with orthorhombic or lower symmetry systems are produced (Bakulin, Grechka and Tsvankin 2002). Verdon, Kendall and Wüstefeld (2009) have generated a method to account for these effects, inverting splitting measurements made on induced microseismic data for the strike and density of sets of aligned fractures and the strength of a VTI sedimentary fabric.

Most studies, in both regional (e.g., Keir *et al.* 2005) and reservoir (e.g., Horne *et al.* 1997; Teanby *et al.* 2004a) seismic settings use SWS to image only one set of fractures. It is usually assumed that ψ, rotated into geographical coordinates, matches the fracture strike and δV_S corresponds to the fracture density, with increasing δV_S corresponding to increasing fracture density. However, it is common for rocks to contain more than one set of aligned fractures. As the presence of a VTI fabric will complicate the anisotropy of a single vertical fracture set, multiple vertical fracture sets will also lead to more complicated anisotropy systems, where simply measuring the fast direction of a subvertically propagating S-wave will not provide sufficient information to characterize the rock.

To do a good job of interpreting SWS measurements, it is necessary to use a rock physics framework to generate elastic stiffness models that can predict S-wave splitting for an arbitrary direction of propagation through an anisotropic rock containing a pre-defined number of aligned fracture sets and a VTI fabric. Such models can be used to create SWS predictions, which can then be compared with the observed splitting measurements. The rock physics model that best matches the observed data is deemed to be the most appropriate. This type of approach has been followed by a number of authors (e.g., Horne and MacBeth 1994; Horne *et al.* 1997; Holmes, Crampin and Young 2000; Rial, Elkibbi and Yang 2005; Verdon *et al.* 2009).

INVERSION APPROACH

Our approach is described in detail in Verdon *et al.* (2009) but we reproduce the key aspects here. To model the slowness surface, **p**, and polarization, **g**, of any body wave propagating through an anisotropic material in an arbitrary direction we use the Christoffel equation,

$$\left(C_{ijkl}\, p_j\, p_k - \rho\delta_{il}\right) g_l = 0, \tag{1}$$

where **C** is the $3 \times 3 \times 3 \times 3$ stiffness tensor, ρ is the rock density and δ_{ij} is the Kronecker delta. Therefore we must develop a rock physics model that is capable of representing a rock mass containing sets of aligned fractures in the form of a stiffness tensor. We use as our basis the additional compliance approach of Schoenberg and Sayers (1995) as described by Hall and Kendall (2000). This method works in the compliance, **S**, domain, where $\mathbf{S} = \mathbf{C}^{-1}$. The overall compliance of the fractured rock system is given by the compliance of the undamaged rock, added to which is the additional compliance imparted by n sets of aligned fracture sets,

$$\mathbf{S} = \mathbf{S^r} + \Delta\mathbf{S^1} + \Delta\mathbf{S^2} + \ldots + \Delta\mathbf{S^n}. \tag{2}$$

The rock frame need not be isotropic and Verdon *et al.* (2009) used a VTI system to describe $\mathbf{S^r}$, with the strength of the S-wave anisotropy given by Thomsen (1986)s γ and δ parameters. The additional compliance approach is particularly well suited to this problem because of the ease with which the effects of multiple fracture sets can be added in a cumulative fashion. The additional compliance tensor for an ith aligned fracture set, if their normals are parallel to the x_1 axis, is given in contracted Voigt notation, by

$$\Delta\mathbf{S^i} = \begin{pmatrix} B_N^i & 0 & 0 & 0 & 0 & 0 \\ 0 & 0 & 0 & 0 & 0 & 0 \\ 0 & 0 & 0 & 0 & 0 & 0 \\ 0 & 0 & 0 & 0 & 0 & 0 \\ 0 & 0 & 0 & 0 & B_T^i & 0 \\ 0 & 0 & 0 & 0 & 0 & B_T^i \end{pmatrix}, \tag{3}$$

where B_N^i and B_T^i are the normal and tangential compliances of the ith fracture set. The additional compliance tensor for each fracture set can be computed in such a manner, before being rotated to the desired strike and dip. The compliance tensors of the undamaged rock frame and each fracture set are added to give the overall compliance, which is inverted to give **C**. The fracture normal and tangential compliances are computed using the equations given by Hudson, Liu and Crampin (1996), using the low-frequency endmember, such that the compliance of a fracture set is a function of only the fracture density (ξ^i) and the Lamé parameters of the

background undamaged rock frame:

$$B_N^i = \frac{4}{3}\left(\frac{\xi^i}{C_{66}^r}\right)\left(\frac{C_{11}^r}{C_{11}^r - C_{66}^r}\right), \quad (4)$$

$$B_T^i = \frac{16}{3}\left(\frac{\xi^i}{C_{66}^r}\right)\left(\frac{C_{11}^r}{3C_{11}^r - 2C_{66}^r}\right). \quad (5)$$

At the low-frequency limit, pore pressure gradients between the fractures and equant pores, induced by the passage of the seismic waves, are completely equalized by movement of fluid. As such, the fluids within the fractures are not able to resist deformation and therefore do not contribute to the stiffness of the fracture. This assumption is appropriate because seismic waves in general have low frequencies, and because by making this assumption we are able to focus on the key first-order parameter, ξ, without having to consider other parameters, such as rock permeability, fluid compressibility and viscosity and fracture aperture, to which SWS is less sensitive. The Hudson (1981) model is one of the simplest fracture models, yet has been widely and successfully used, especially when the low-frequency endmember, developed in Hudson *et al.* (1996), is considered. The interested reader is directed towards Pointer, Liu and Hudson (2000) and Hall and Kendall (2000) for reviews and further discussion of the most commonly available fracture models in the literature.

The approach outlined by Verdon *et al.* (2009) provides a simple rock physics model where the elastic stiffness tensor depends on a limited number of parameters, all useful to a reservoir engineer: Thomsen's parameters to describe a VTI sedimentary fabric (γ, δ) and the densities and strikes of any number of aligned vertical fracture sets (ξ^i, α^i). Verdon *et al*'s. (2009) inversion procedure used a grid search method to explore the parameter space, comparing observed SWS parameters (δV_S, ψ) for each recorded shear-wave arrival with forward modelled values computed using the Christoffel equation. We normalize the rms misfit surfaces for both δV_S and ψ by their respective minima, before combining them to give the overall misfit. The minimum of this misfit surface gives the best fit rock physics model to describe the observed SWS. We use an F-test to compute the 90% confidence interval (see, e.g., Silver and Chan 1991). When plotting the misfit surfaces, we normalize the misfit values such that the 90% confidence interval is equal to 1 (marked in bold in Figs 2, 3, 5–7). This limit allows us to infer the accuracy of an inversion – a tight confidence ellipse implies a well constrained result.

Sophisticated inversion mechanisms can be used to find the best fit result, although the objective function to be minimized remains the difference between observed splitting measurements and those modelled using rock physics methods. However, the simplicity of the rock physics model means that a grid search based routine can provide sufficiently detailed coverage of the parameter space without being overly demanding computationally. It would also be possible to weight the misfit surfaces for ψ and δV_S such that one is favoured by the inversion, for instance if one parameter was more precisely measured. However, we do not treat them as such in this paper.

The purpose of this paper is to demonstrate how the presence of several fracture sets can be identified using SWS. We begin by demonstrating the observation of multiple fracture sets at the Weyburn CCS-EOR site in Canada. We follow this by showing that it is possible to discriminate when only a single fracture set is present, using data from a hydraulic fracture job. Finally, we will generate synthetic data to demonstrate how the assumption that only one fracture set is present, when in fact there are multiple sets, can lead to problems if the range of shear-wave propagation directions is not broad enough.

WEYBURN

The Weyburn CCS-EOR site has been injecting CO_2 since 2000 for commercial EOR, as well as an opportunity to test various monitoring techniques for carbon capture and storage. A downhole microseismic monitoring array was installed in 2003 to monitor the injection in one of the 19 patterns. The array of 8 triaxial geophones was placed in a vertical well near to the vertical injection well. Several horizontal production wells are nearby. The geophones were placed just above the reservoir depth and began recording in August 2003. CO_2 injection was initiated in January 2004. 68 events were recorded, the majority of which occurred after injection began. Event locations are plotted in Fig. 1.

More details on the microseismic monitoring program at Weyburn can be found in White (2009) and on the SWS measurements in Verdon (2010) and Verdon *et al.* (2010b). The SWS measurements were made using the semi-automated algorithm described by Teanby, Kendall and van der Baan (2004b). Of the 544 possible SWS measurements (68 events × 8 geophones) only 30 provided reliable measurements according to the Teanby *et al.* (2004b) criteria, a relatively low rate of success for SWS analysis. This reflects the fact that the signal-to-noise ratio for the data is not particularly good.

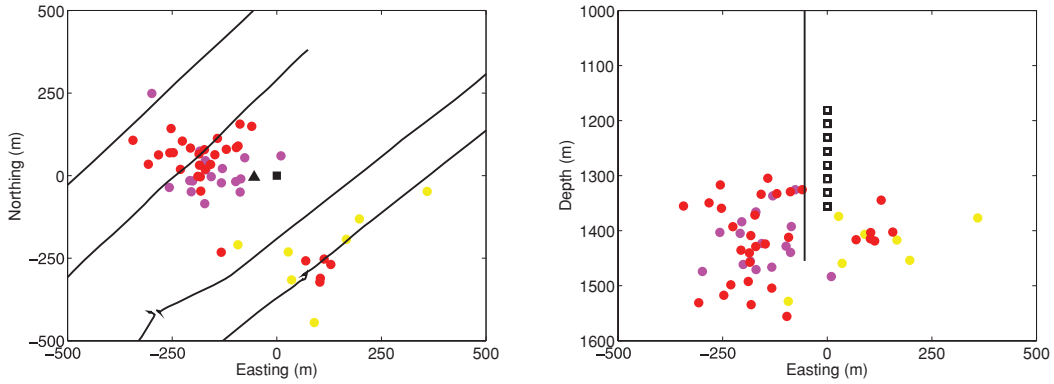

Figure 1 Map view (a) and cross-section (b) of microseismic events detected at Weyburn. The injection well is marked in (a) by the solid black triangle, and the monitoring well by the solid square. Nearby horizontal production wells are marked by black lines. In (b), the injection well is marked by the black line, which terminates at the injection depth, while the geophones are marked by squares. Events are coloured by temporal clusters - yellow = event occurring before injection, magenta = events occurring during CO_2 injection between January-April 2004, red = events occurring during a period of increased injection rate in May-July 2004.

Inversion for one fracture set

The SWS measurements are plotted in Fig. 2(a) (green-outlined ticks). This azimuthal equidistant upper hemisphere projection maps the arrival azimuths and inclinations of the S-waves that provided good measurements (tick location) and shows the measured ψ (tick orientation) and δV_S (tick colour and length). We begin by inverting these measurements for one set of aligned fractures and a VTI sedimentary fabric. The unknown parameters in the inversion are ξ^1, α^1, γ and δ. The results of the inversion are given in Table 1 and plotted in Fig. 2. When one fracture set is modelled, the inversion finds that the best fitting model has fractures striking at 138°. The rms misfit surfaces as a function of fracture strike, fracture density and γ are also plotted. When plotting the misfit as a function of strike, we use polar coordinates, where the polar angle gives fracture strike and the radial axis gives fracture density. For this result, the 90% confidence interval (bold contour) is large, suggesting that the inversion has not found a particularly well fitting result.

Core analysis and borehole image logs at Weyburn have indicated the presence of aligned fracture sets at Weyburn (Bunge 2000; Brown 2002). Two of the fracture sets identified by these studies are listed in Table 1. These sets have strikes of 40° and 148°, with the set at 40° being the more pervasive. However, our SWS inversion has identified the apparently weaker set at 138°. One reason for this may be the geometry of the arrivals available to conduct the inversion. Verdon *et al.* (2009) have shown that features that are resolvable with SWS measurements are highly dependent on the direction of ray propagation relative to them. Splitting will be maximum when an S-wave travels in the plane of a fracture set and will be zero when the wave travels perpendicular to the fractures. The events at Weyburn are located predominantly to the NW and SE of the recording array (Fig. 1a). As such the emitted shear waves will travel subparallel to fractures striking NW-SE and subperpendicular to fractures striking NE-SW. Because of this orientation of sources, receivers and structures, it is the fracture set striking to the NW-SE that is preferentially imaged.

Inversion for two fracture sets

We run a second inversion to find the strike and density of two vertical fracture sets. Because the inversion with one fracture set did not find a well constrained or significant VTI fabric, we do not assume any for this second inversion. The unknown parameters in this inversion were ξ^1, α^1, ξ^2 and α^2. Before showing the results of the inversion we note a discrepancy between our results for VTI fabric and the VTI fabric found by Bellefleur, White and Davis (2004) and Bellefleur *et al.* (2003). In the results presented below we use the weak VTI parameters computed by our inversion for 1 fracture set. For the deepest reflector they studied (at 1400 m), Bellefleur *et al.* (2004) found $\epsilon = 0.06$ and $\delta = 0.02$. We note that substituting these values (Bellefleur *et al.* (2004) did not compute γ, so we assume $\gamma = \epsilon$) for the strength of VTI fabric does not change the results of the 2-fracture inversion. The discrepancies in anisotropic parameters between our study and those found

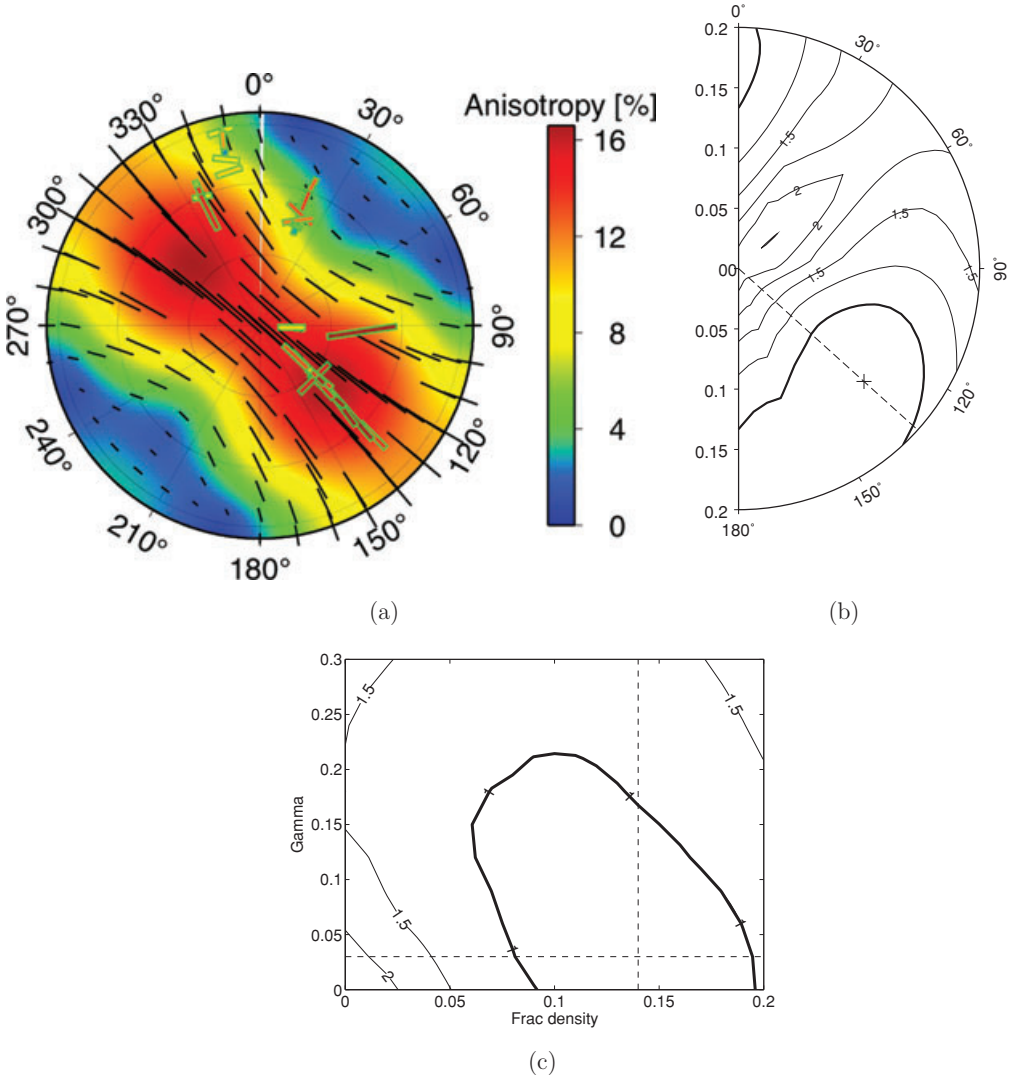

Figure 2 Inversion results for the SWS measured at Weyburn assuming only 1 fracture set. In (a) we show an azimuthal equidistant upper hemisphere projection of the observed splitting results at Weyburn (green-outlined ticks). The position of the tick marks the arrival azimuth and inclination of the S-wave. The orientation of the tick marks ψ, while the length of the tick, and its colour, give δV_S. Also plotted, with thin black ticks and contours, is the modelled splitting using the best fit parameters. The thin ticks give the modelled ψ, while the contours give the modelled δV_S. In (b) and (c) we show the misfit surface computed by the inversion, as a function of fracture strike (α) and density (ξ), and the VTI strength (γ), normalised such that a value of 1 equals the 90% confidence interval. In (b), the misfit contours are shown on a polar plot, where the radial axis gives the fracture density, and the polar angle gives fracture strike. The bold contour shows the 90% confidence interval. The inversion finds a best fit fracture set with a strike of 138° and a density of 0.14.

by Bellefleur *et al.* (2003) and Bellefleur *et al.* (2004) are discussed in more detail below. The inversion finds fractures striking at 42° and 150° (Fig. 3). In particular, we note in Fig. 3(d,e) the misfit surfaces clearly show the need for two fracture sets whose strikes are close to orthogonal to each other. The 90% confidence intervals for the strikes of the two sets do not overlap at any point.

The fracture orientations provide a good match with the fractures identified in core samples and borehole image log analysis, indicating that the method has been successful (Table 1). When we examine the misfit surfaces, we note that the best fit fracture densities trade off against each other (Fig. 3b) – this is because the two fracture set orientations are close to orthogonal. Grechka and Tsvankin (2003) and

Table 1 Results for the inversion of Weyburn SWS measurements assuming 1 and then 2 fracture sets are present. We also give the results of core and borehole analysis at Weyburn provided by Brown (2002). The fracture densities in this study are given by Hudson (1981)'s nondimensional fracture density term, but in Brown (2002) they are written as the number of fractures per meter of rock

	ξ^1	α^1	ξ^2	α^2	γ	δ
Inversion for 1 fracture set	0.14	138°	N/A	N/A	0.03	0.0
Inversion for 2 fracture sets	0.3	150°	0.21	42°	N/A	N/A
From Brown (2002)	1.0–1.6 m^{-1}	148°	2.3–3.8 m^{-1}	40°	N/A	N/A

Bakulin *et al.* (2002) have shown that the same stiffness tensor, **C** and therefore the same SWS patterns, can be produced by a range of fracture densities, so long as the fractures are close to orthogonal. This means that the absolute value of fracture density for the two sets is not uniquely resolvable. However, we can determine the relative strength of each set: in Fig. 3(b) the 90% confidence interval shows that the best fit fracture density for the set at 150° must be larger than the density of the set at 42°. This is in disagreement with the core sample work, which finds that the set at 40° has a higher density. We note at this point that in Table 1 we are not quite comparing like with like, because fracture spacing need not necessarily correlate with the overall compliance of a fracture set. Furthermore, there may well be geomechanical reasons for this disagreement (Verdon *et al.* 2010b), with injection activities altering the stress conditions to preferentially open the set at 150° (which runs perpendicular to the horizontal well trajectories at Weyburn). The influence that stress changes have on seismic anisotropy, by forcing open or closed fractures and microcracks with certain orientations, has been documented by e.g., Tod (2002), De Meersman, Kendall and Van der Baan (2009), Teanby *et al.* (2004a) and Verdon *et al.* (2008).

A 9-component (triaxial geophones, shear and compressional sources) VSP survey was also conducted to image the anisotropy at Weyburn (Bellefleur *et al.* 2003, 2004). We note that this VSP survey is located over 2 km from the microseismic survey discussed here. Nevertheless it is interesting to compare their findings with our observations under the assumption that there is lateral continuity between the surveys. Bellefleur *et al.* (2003) found that the anisotropy is dominated by a VTI fabric and to a lesser extent by N-S striking fractures. This is in stark contrast to our work, which images fracture sets striking NW-SE and NE-SW and little VTI fabric (although γ is not well constrained in our inversion). This discrepancy might highlight the advantage of using SWS measured on microseismic surveys. Because SWS is a path-averaged effect, the SWS results collected by Bellefleur *et al.* (2003) gave the 'net' anisotropy of the whole overburden from the surface sources to the geophone at 1340 m depth. As such, they do not pertain to the reservoir (at a depth of 1430 m). This is further corroborated by the fact that Bellefleur *et al.* (2003) found that much of the anisotropic system observed at 1340 m had already established itself by 900 m depth, suggesting that the SWS measured by Bellefleur *et al.* (2003) was generated by rocks a long way from what we are most interested in. Our SWS measurements are made on events located in, under and immediately above the reservoir and recorded on geophones above the reservoir. As such our SWS measurements can be attributed to the reservoir and the immediate caprock (which is trapping the injected CO_2). These measurements will be of much greater interest for reservoir characterisation, neatly demonstrating the advantage of measuring SWS on microseismic events located in and around the reservoir and detected on geophones near the reservoir. It is telling that our SWS measurements provide a good match with independent estimates of reservoir properties: no VTI anisotropy has been measured on reservoir core samples (this of course does not preclude VTI anisotropy generated by thin layering) and VTI anisotropy is generally less common in carbonate compared to clastic rocks (the Weyburn reservoir consists of limestone and dolostone parts). Furthermore, our fracture strikes match the strikes of fracture sets identified in core samples.

HYDRAULIC FRACTURING

The second data set we use comes from a hydraulic fracture job conducted in a producing North American oilfield. This data set has been discussed in more detail by Verdon, Kendall and Maxwell (2010a). Confidentiality agreements limit the available geological information about this field. The fracture was stimulated in the reservoir from a vertical injection well and microseismic events were recorded on an array of

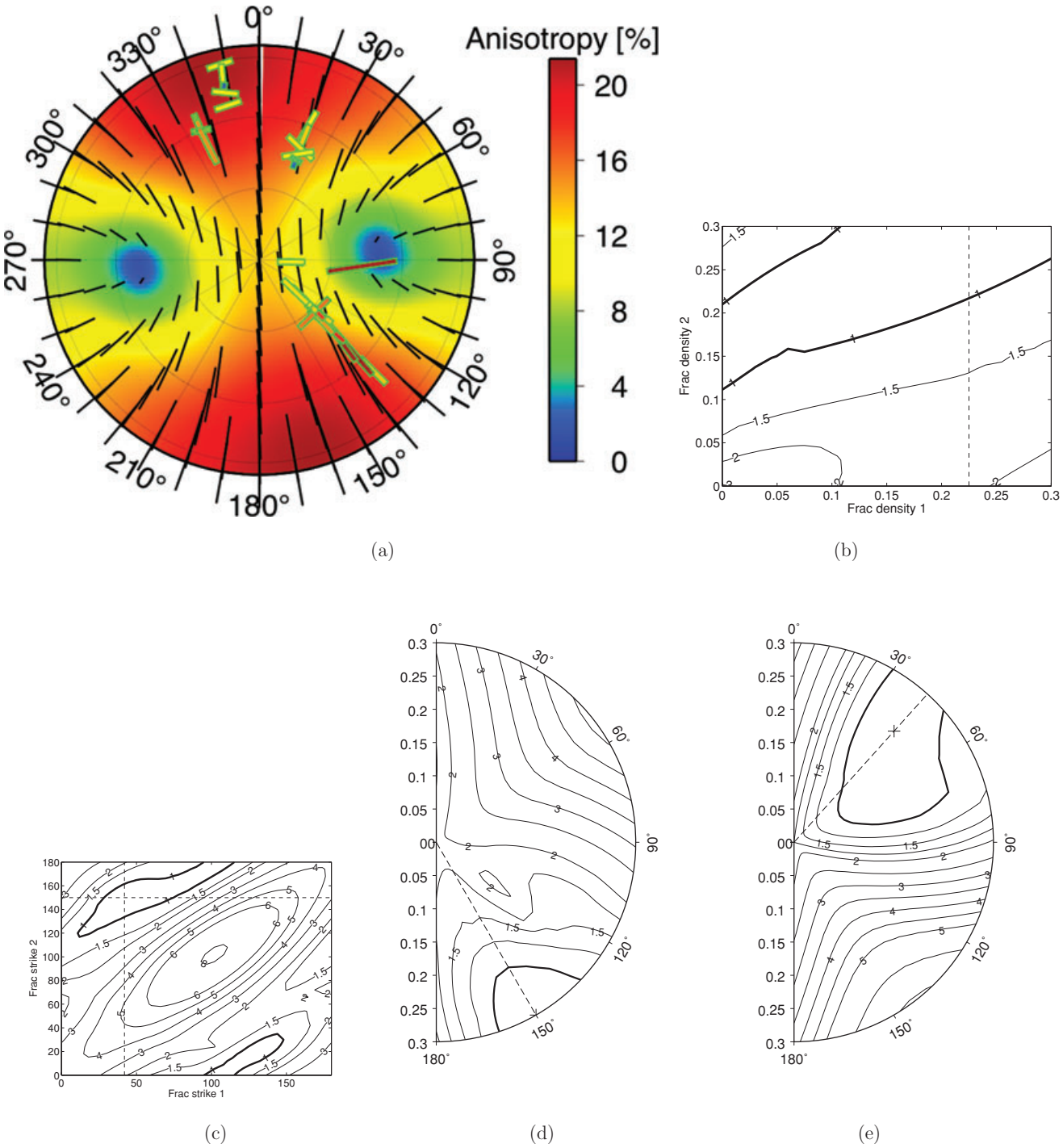

Figure 3 Inversion results for the Weyburn SWS measurements using two fracture sets. In (a) we show an upper hemisphere plot of the SWS measurements in the same format as Fig. 2a. In (b) we show the misfit surface as a function of the fracture densities, and (c) shows the misfit surface as a function of the fracture strikes. The inversion finds two fracture sets with strikes of 150° and 42°. The fracture densities are poorly constrained because they trade off against each other, but the 2nd set, with a strike of 150°, is always the more dominant. Panels (d) and (e) show the misfit as a function of the fracture densities and strikes of each set, using the polar plotting convention described in Fig. 2.

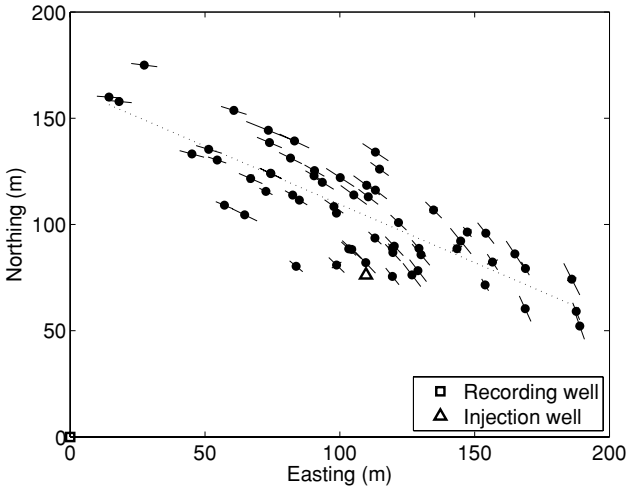

Figure 4 Map view of event locations during the hydraulic fracture job. The vertical monitoring well is at (0,0), and the injection well is marked. The events track the formation of fractures trending at 120° from the injection well.

12 triaxial geophones in a nearby vertical observation well. The geophones were placed at reservoir depths, meaning that the recorded energy has travelled subhorizontally. The event locations detected during fracturing are plotted in Fig. 4. The event locations track the formation of fractures striking at an azimuth of 120° away from the injection well.

Inversion for one fracture set

The SWS measurements made during this fracture stimulation are discussed in more detail in Verdon (2010), Verdon *et al.* (2009) and Verdon *et al.* (2010a). The measurements are made using the semi-automated Teanby *et al.* (2004b) algorithm, and of the 780 potential measurements (65 events × 12 geophones), 45 were deemed to be of the highest quality. The measurements are plotted in Fig. 5(a) in the same format as for the Weyburn data. The majority of the fast directions are orientated subhorizontally, indicating the importance of a VTI fabric in the anisotropic system. These data were inverted for one fracture set and a VTI fabric by Verdon *et al.* (2009) and we reproduce the results here (Fig. 5), listing the best fit parameters in Table 2. The unknown parameters in this inversion were ξ^1, α^1, γ and δ. The inversion finds $\gamma = 0.04$, $\delta = 0.1$, and fractures striking at 120°. The fracture strike found by the inversion provides an excellent match with the fracture strike observed from the trend of event locations, giving us confidence in the success of the inversion. Synthetic tests using the range of available S-waves (Verdon *et al.* 2009) have shown that, given the restricted range of data and the source-receiver geometry, it will be difficult to image the number density of a fracture set with this orientation. This is borne out by the inversion results where, although γ and α are well constrained, ξ is not.

Inversion for two fracture sets

We now repeat the inversion process but searching for two fracture sets. As our two fracture set inversion does not consider sedimentary fabrics, we fix the strength of γ and δ to the values found for one fracture set. If only one fracture set is present, then the inversion should not require the extra fracture parameters, meaning that the inversion will find that the strikes of both sets are the same (i.e., the two modelled fracture sets with the same strike are in fact one fracture set). The unknown parameters in this inversion are ξ^1, α^1, ξ^2 and α^2.

The results of this inversion are plotted in Fig. 6. The best fit fracture strikes and densities found are given in Table 2. The best fit results for both fracture strikes are close to 120°, and when the rms misfit surfaces are examined as a function of the density and strike of either fracture set (Fig. 6c,d), we note that these surfaces have the same topography. This confirms that only one fracture set is needed to model the observed SWS measurements. Both misfit topographies allow fractures striking at 120° only and of course two fracture sets striking in the same direction are in fact one fracture set whose fracture density is the sum of their individual densities. The densities of the two sets, 0.07 and 0.03, sum to give the density of the original single fracture set, 0.1. This result is to be expected from equations (2), (4) and (5), where the compliances of each fracture set are added to give the overall compliance. This approach ignores second-order fracture-fracture interations, so two fracture sets with the same strike (perhaps of differing scale), generate the same stiffness as one more compliant fracture set with the same strike. The presence of fractures striking at 120° inferred from SWS analysis still matches with the fracture strike as inferred from event locations (Fig. 4).

As well as the principal fracture set, hydraulic fracturing can open secondary, or conjugate, fracture sets with a differing orientation to the main fracture. The dual fracture set inversion for this data set suggests that no such fracture sets have been generated during this fracture job. This information can be identified with accurate event locations and even focal mechanisms (e.g., Rutledge, Phillips and Mayerhofer 2004; Eisner *et al.* 2010) but these types of analyses are difficult to

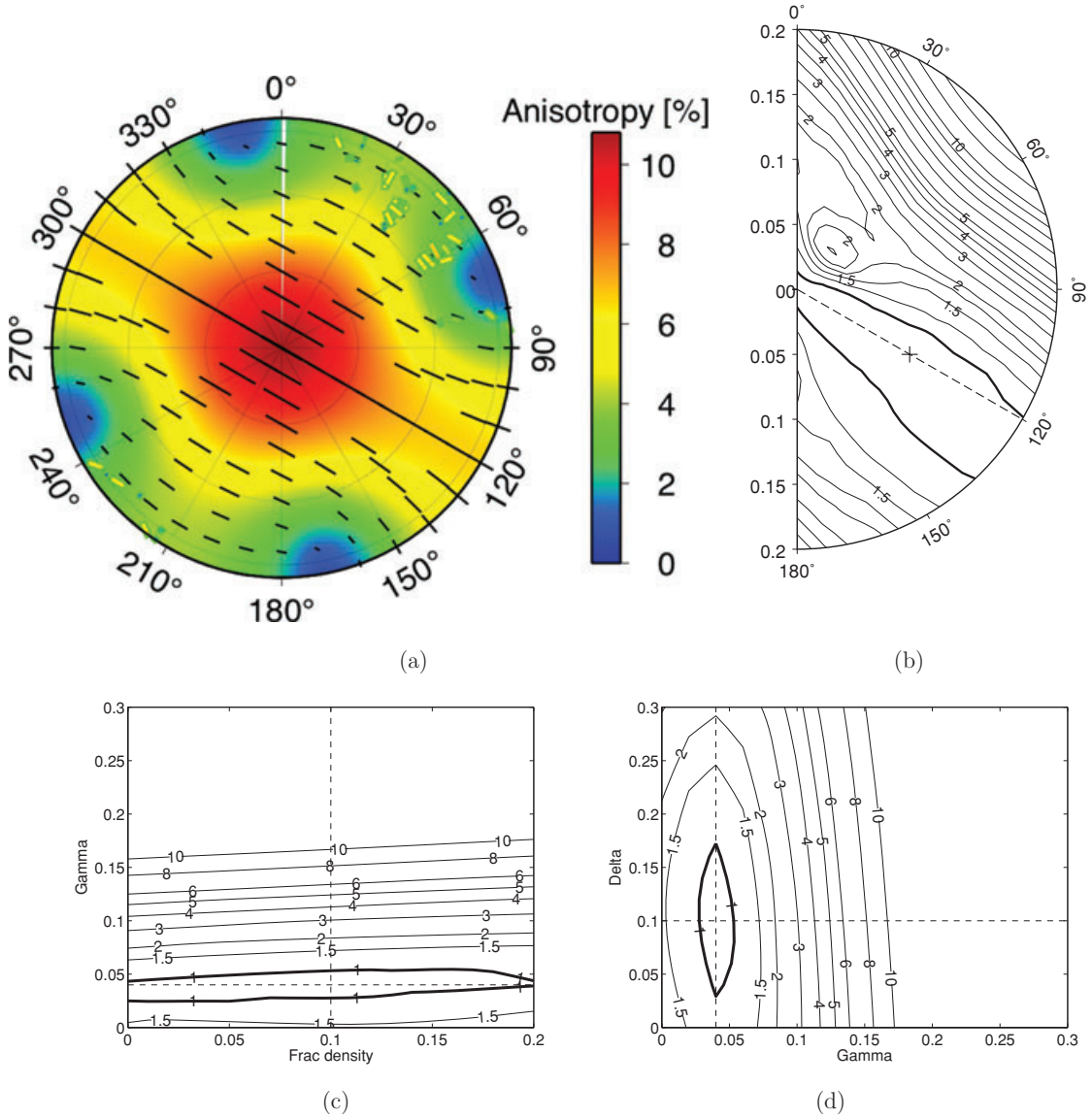

Figure 5 Results for the inversion of SWS measurements on the hydraulic fracture data, assuming 1 fracture set is present along with a VTI fabric. In (a) we show the measurements (green-outlined ticks) and the best fit model (contours and thin ticks). The rms misfit as a function of fracture strike, fracture density and VTI fabric strength (γ and δ) are plotted in (b-d). The inversion finds that $\gamma = 0.04$, $\delta = 0.1$, and that fractures strike at 120°. Fracture density is poorly constrained.

obtain without multiple monitoring wells or very good quality data. This example shows how SWS measurements can be used to help fill this knowledge gap.

VERTICAL ARRIVALS

Commonly, SWS analyses use subvertical arrivals to image vertical fractures (subvertical here is defined arbitrarily as being within 20° of vertical). This is because such observations are the easiest to interpret in terms of vertical fracture sets. With one fracture set, ψ will represent fracture strike and δV_S will correlate with fracture density. However, with two (or more) fracture sets present, this picture will be more complicated. Here we generate a synthetic dataset with such arrivals, assuming a rock mass with multiple fracture sets and by conducting an inversion using only one fracture set, show the pitfalls that can be encountered by doing so.

Table 2 Results for the inversion of the hydraulic fracture SWS measurements assuming 1 and then 2 fracture sets are present. The fracture strikes at 120° match the orientation of the fracture inferred from event locations

	ξ^1	α^1	ξ^2	α^2	γ	δ
Inversion for 1 fracture set	0.1	120°	N/A	N/A	0.04	0.1
Inversion for 2 fracture sets	0.07	117°	0.03	126°	N/A	N/A
Event locations	N/A	120°	N/A	N/A	N/A	N/A

We construct an initial elastic model of a rock containing two sets of fractures, striking at 90° and 20°, with fracture densities of 0.1 and 0.07 respectively. This model is used to generate synthetic SWS data, modelling the fast directions and splitting magnitudes of waves arriving with a range of inclinations between 0–20° from vertical and azimuths between 0–180°. The Christoffel relationship given in equation (1) is used to compute the splitting parameters. Random noise is added to the data, with maximum noise of ±0.5% to δV_S and ±10° to ψ. These represent common error distributions for SWS measurements. With real data, knowledge of the arrival azimuths and inclinations is also subject to uncertainty, so we add random noise of up to ±10° to the raypath orientation as well. This represents the synthetic dataset, from a rock containing two fracture sets, which we will invert assuming only one fracture set, to highlight the pitfalls that can occur. The unknown parameters in this inversion are ξ^1, α^1, γ and δ.

The results of the inversion are shown in Fig. 7. The inversion finds that the data are best fit, assuming only one fracture set, with a set striking at 66° and a density of 0.06. Verdon *et al.* (2009) noted that SWS measurements on subvertical arrivals will struggle to image VTI fabrics and this is borne out in this example, where γ and δ trade off against each other and so are poorly constrained (Fig. 7c). The two fracture sets combine to give the overall anisotropy system, which, for subvertical arrivals at least, can be approximated by one fracture set. When we compare the synthetic data (generated by two fracture sets) and the inversion results (green-outlined and black ticks respectively in Fig. 7a) we note a good match. When we examine the topography of the misfit surface (Fig. 7b) we note that the inversion has found a stable, well fitting result. This indicates that for subvertical arrivals the SWS generated by two vertical fracture sets is no different to a one set with an intermediate strike. This means that it will not be possible to distinguish when multiple fracture sets are present. When multiple sets are present, measurements of ψ will represent the strike of neither fracture set but an intermediate direction instead. Only when a wider range of S-wave arrival inclinations are used, including S-waves that have travelled sub-horizontally, can two separate fracture sets be identified accurately with no ambiguity.

This is a potential pitfall when using SWS from only subvertical arrivals – it can be easy to mistake what appears to be a simple case of one fracture set, when in fact two sets are combining to give the overall anisotropy. A wider range of arrivals, including subhorizontal arrivals, is needed to properly characterize the anisotropy. SWS measurements made using 9-C reflection surveys will often not achieve this range, especially for deeper reflectors. However it should be noted that other observable features of 9-C surveys, particularly azimuthal AVO and NMO variations, can be used to image fractures (e.g., Bakulin *et al.* 2000; Grechka and Tsvankin 2003). Microseismic events represent an excellent shear wave source, because with a suitably placed recording array they can provide horizontally propagating shear waves that will be helpful to constrain the anisotropic symmetry system. Synthetic tests such as the one presented here can help constrain what structures can and cannot be imaged with the arrivals available and can also be used to guide geophone locations to maximize what can be imaged with SWS.

DISCUSSION

Shear-wave splitting has demonstrated potential for imaging aligned fabrics in a reservoir. However, the interpretation of splitting results is not trivial. Care needs to be taken when using raw SWS data to infer the orientations and strengths of aligned fracture sets and sedimentary fabrics. Commonly, the arithmetic average of fast directions, rotated from ray frame to geographical coordinates, is assumed to give the strike of the principal fracture set. This work has shown not only the pitfalls that can be found by doing so but also the information that can be gained by interpreting SWS data in a more rigorous manner. By generating rock physics models with which to forward model splitting, it should be possible to image multiple fabrics in the reservoir.

The ability to differentiate between one or more fracture sets will be of great use for reservoir management, particularly as the industry looks to explore more unconventional hydrocarbon resources, such as tight gas, shale gas and coal bed methane, which require fractures – either natural or stimulated – to produce. However, a good range of arrival azimuths and inclinations is needed to constrain the overall anisotropy

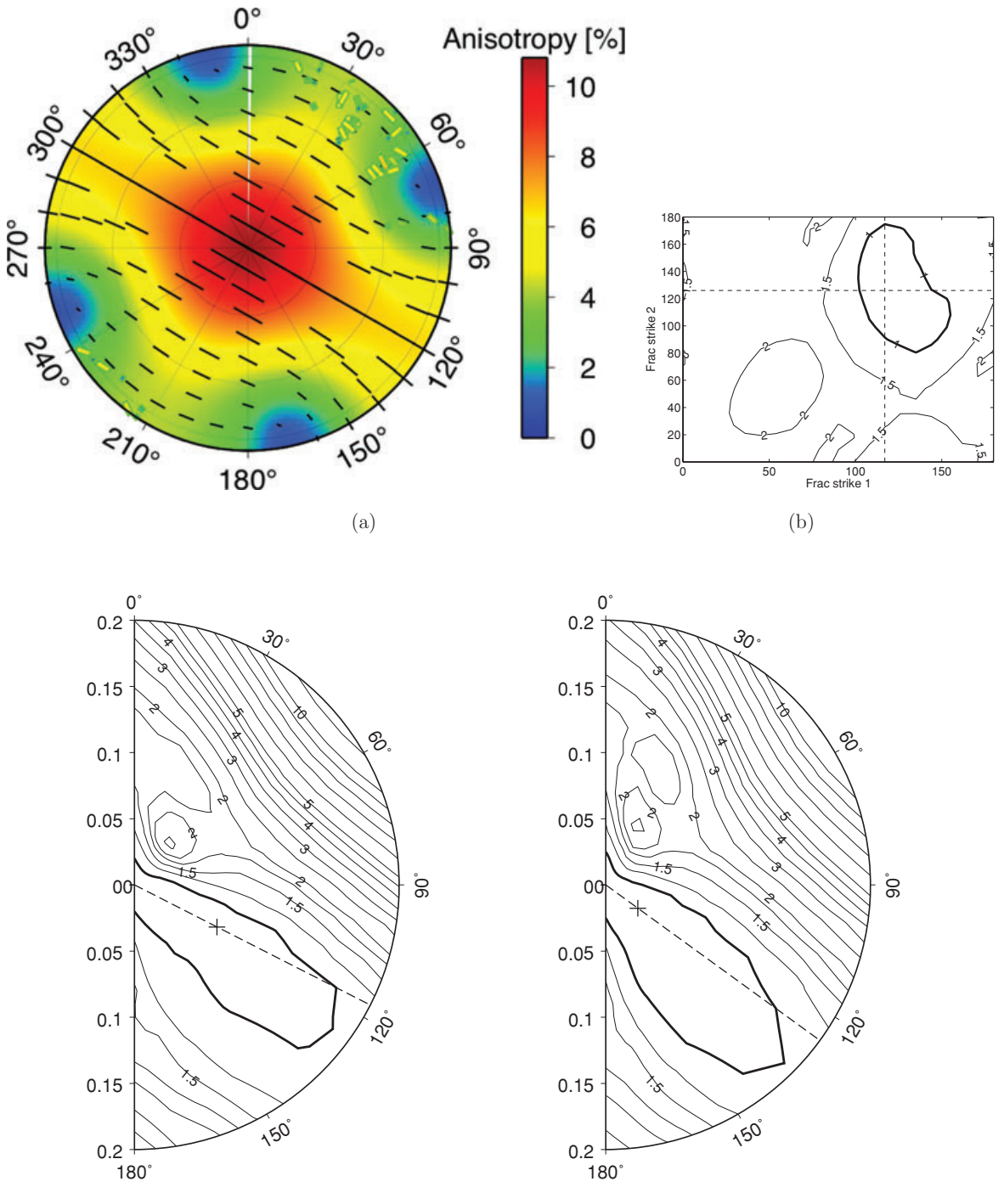

Figure 6 SWS inversion results for the hydraulic fracture assuming two fracture sets. In (a) we show an upper hemisphere projection of the measurements and best fit model as in previous figures. In (b) we show the misfit as a function of the two fracture strikes, both of which center on 120°. We show the misfit as a function of the first (c) and second (d) fracture set strikes and densities, with density as the radial axis and strike as the polar angle. The misfit topographies in (c) and (d) are essentially identical, demonstrating that only one fracture set, with a strike of 120°, is needed to model the observed SWS.

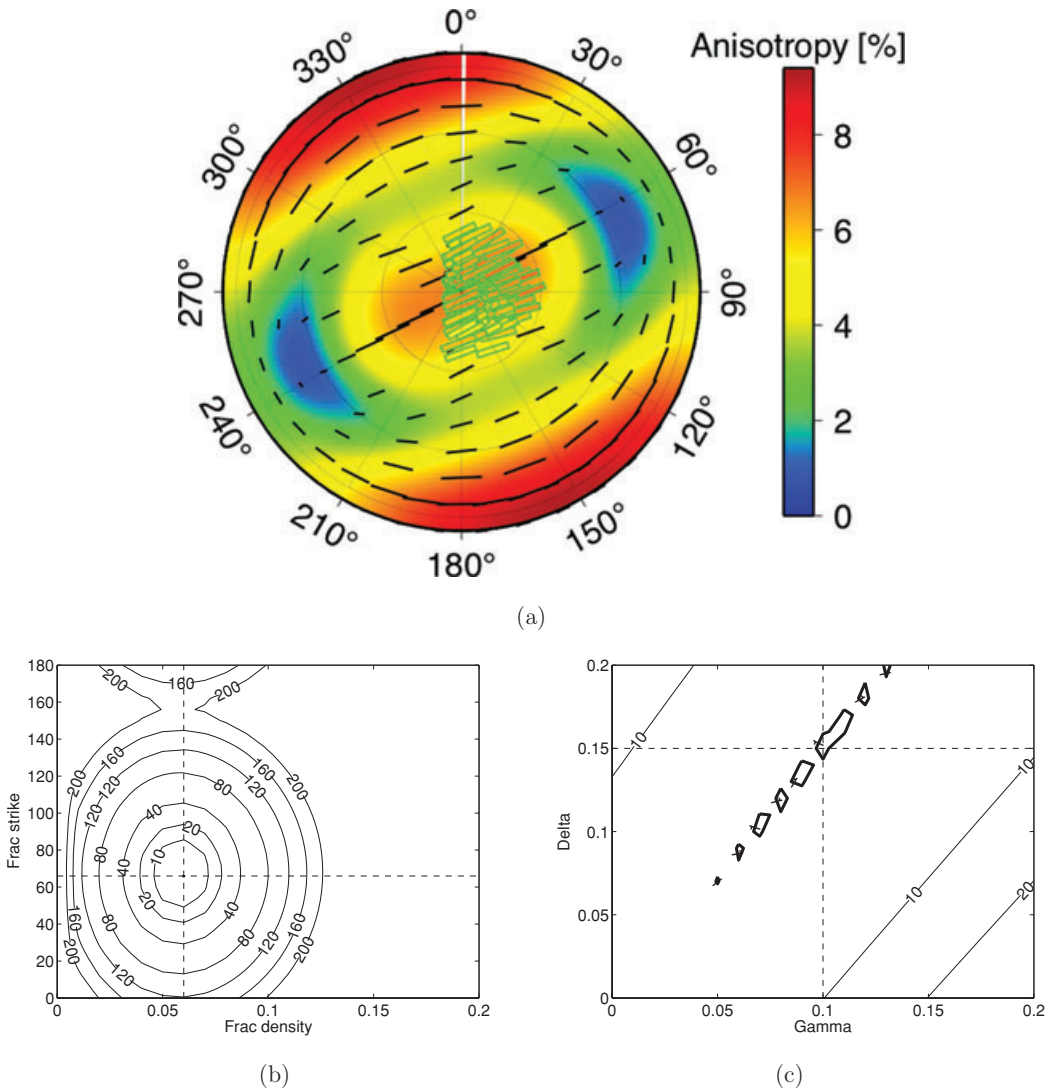

Figure 7 SWS inversion results for the synthetic dataset with vertical arrivals. In (a) we plot the synthetic data (broad ticks) and the best fit model assuming only one fracture set (thin ticks and contours). In (b) we plot the rms misfit as a function of the strike and density of the one fracture set used in the inversion, and in (c) we show that for subvertical arrivals γ and δ trade off against each other and are poorly constrained.

system. We have shown with our synthetic example that a limited range of arrivals, even if they are subvertical, may not be sufficient to properly characterize the anisotropy. Synthetic modelling can be used to predict the range of arrivals needed to image a particular structure and which raypaths will be the most effective in doing so. If it is known where microseismic events are likely to occur – for instance if a frac-job is planned, or using geomechanical models (e.g., Angus *et al.* 2010; Verdon *et al.* 2010b) – then this capability can be used to make decisions on where to place geophones to maximize what can be imaged using SWS.

Our paper assumes that the shear waves have travelled through a medium with constant anisotropy throughout. Significant spatial variation in anisotropy along a raypath, or between raypaths, may cause the inversion technique to break down. In such a situation, shear-wave splitting tomographic techniques (e.g., Abt and Fischer 2008; Wookey 2010) can be used to resolve regions with differing anisotropy. However, without large volumes of data, the number of free parameters needed for such techniques will tend only to introduce trade-offs and non-uniqueness to the solutions, rather than an improved solution. Our approach also has an advantage in its

much reduced computational requirements (the tomographic technique of Wookey (2010) requires a cluster to perform the computations).

CONCLUSIONS

We have developed a method for inverting SWS measurements made on microseismic data for the presence of multiple aligned fracture sets. This method uses a rock physics based approach, where elastic stiffness tensors are constructed. By using the Christoffel equation, SWS can be predicted from such stiffness tensors. These modelled splitting values provide the forward models with which the observed data can be compared and by minimizing the misfit between model and observations a best fit model can be found.

Commonly, it is assumed that anisotropy is caused by a single aligned fracture set, potentially combined with VTI sedimentary fabrics. However, it should be possible to use SWS to detect more than one fracture set. We demonstrate this using SWS measurements made on microseismic data from the Weyburn CCS site. Core and borehole analysis has indicated the presence of multiple fracture sets in the Weyburn reservoir, so this provides an excellent opportunity to test whether multiple sets can be imaged. Our initial inversion, for one fracture set, did not find a particularly satisfactory best fit model. A second inversion for two fracture sets successfully finds two fracture sets whose strikes match well with the fractures identified in core samples and borehole image log work.

It is also of use to evaluate whether there is one or more fracture sets present. To demonstrate this we use a second dataset from a hydraulic fracture. Our inversion finds a suitable result using one fracture set only. When a second fracture set is added to the inversion, it is found to be unnecessary. This indicates that only one fracture set has been stimulated by the hydraulic fracturing. The capability of shear-wave splitting analysis to distinguish the number of fracture sets present will be very useful when conducting frac-jobs.

We have also demonstrated the pitfalls that can be encountered when dealing with subvertical arrivals when more than one fracture set is present. A synthetic splitting dataset is generated for a rock with two fracture sets illuminated by subvertical arrivals. This dataset is then inverted assuming only one fracture set is present. The inversion finds a well constrained best fit model but the strike of the inverted fracture set does not match the strike of either of the input fracture sets, while the fracture density found by the inversion is lower than the density of either of the input fracture sets. This paper demonstrates the need for a wide a range of arrivals as possible and a suitable rock physics based inversion approach, when interpreting SWS measurements. However, it also shows that, with suitable data and a rigorous inversion method, multiple fracture sets can be imaged. At present, SWS measurements on microseismic data is a technique still in its infancy. As such, it is important to compare SWS observations with independent characterizations of the reservoir – by doing so the effectiveness (or otherwise) of the technique can be demonstrated. If the technique can be shown to provide useful information, it will be relatively easy to adopt it wherever microseismic events are detected, as automation procedures exist to measure and analyse large volumes of data relatively quickly (e.g., Teanby *et al.* 2004b; Verdon *et al.* 2009; Wüstefeld *et al.* 2010).

ACKNOWLEDGMENTS

The authors would like to thank Pinnacle Technologies Ltd for providing the hydraulic fracture data and PTRC for providing the Weyburn microseismic data. This work was conducted as part of the Bristol University Microseismicity ProjectS (BUMPS). We also thank the anonymous reviewers whose comments helped improve the quality of the paper.

REFERENCES

Abt D.L. and Fischer K.M. 2008. Resolving three-dimensional anisotropic structure with shear wave splitting tomography. *Geophysical Journal International* **173**, 859–886.

Angus D.A., Kendall J.-M., Fisher Q.J., Segura J.M., Skachkov S., Crook A.J.L. and Dutko M. 2010. Modelling microseismicity of a producing reservoir from coupled fluid-flow and geomechanical simulation. *Geophysical Prospecting* **58**, 901–914.

Bakulin A., Grechka V. and Tsvankin I. 2000. Estimation of fracture parameters from reflection seismic data – Part I: HTI model due to a single fracture set. *Geophysics* **65**, 1788–1802.

Bakulin A., Grechka V. and Tsvankin I. 2002. Seismic inversion for the parameters of two orthogonal fracture sets in a VTI backgroound medium. *Geophysics* **67**, 292–299.

Barruol G. and Hoffmann R. 1999. Upper mantle anisotropy beneath the Geoscope stations. *Journal of Geophysical Research* **104**, 10757–10774.

Bellefleur G., Adam L., White D.J., Mattocks B. and Davis T.L. 2003. Seismic imaging and anisotropy analysis of 9C 3D-VSP data at Weyburn Field, Saskatchewan, Canada. 73rd SEG meeting, Dallas, Texas, USA, Expanded Abstracts, 1326–1329.

Bellefleur G., White D.J. and Davis T.L. 2004. P-wave imaging using 3D-VSP data in VTI media, Weyburn Field, Saskatchewan Canada. 74th SEG meeting, Denver, Colorado, USA, Expanded Abstracts, 2521–2524.

Blackman D.K. and Kendall J.-M. 1997. Sensitivity of teleseismic body waves to mineral texture and melt in the mantle beneath a

mid-ocean ridge. *Philosophical Transactions of the Royal Society of London A* **355**, 217–231.

Blackman D.K., Orcutt J.A., Forsyth D.W. and Kendall J.-M. 1993. Seismic anisotropy in the mantle beneath an oceanic spreading center. *Nature* **366**, 675–677.

Boness N.L. and Zoback M.D. 2006. Mapping stress and structurally controlled crustal shear velocity anisotropy in California. *Geology* **34**, 825–828.

Brown L.T. 2002. *Integration of rock physics and reservoir simulation for the interpretation of time-lapse seismic data at Weyburn field, Saskatchewan*. Master's thesis, Colorado School of Mines.

Bunge, R.J., 2000. *Midale reservoir fracture characterization using integrated well and seismic data, Weyburn field, Saskatchewan*. Master's thesis, Colorado School of Mines, Golden, Colorado.

Crampin S. 1991. A decade of shear-wave splitting in the Earth's crust: what does it mean? what use can we make of it? and what should we do next? *Geophysical Journal International* **107**, 387–407.

Crampin S., Gao Y. and Peacock S. 2008. Stress-forcasting (not predicting) earthquakes: A paradigm shift? *Geology* **36**, 427–430.

Crampin S. and Peacock S. 2008. A review of the current understanding of seismic shear-wave splitting in the earth's crust and common fallacies in interpretation. *Wave Motion* **45**, 675–722.

Davis T.L., Terrell M.-J., Benson R.D., Cardona R., Kendall R.R. and Winarsky R. 2007. Multicomponent seismic characterization and monitoring of the CO^2 flood at Weyburn Field, Saskatchewan. *The Leading Edge* **22**, 696–697.

De Meersman K., Kendall J.-M. and Van der Baan M. 2009. The 1998 Valhall microseismic data set: An integrated study of relocated sources, seismic multiplets and S-wave splitting. *Geophysics* **74**, B183–B195.

Eisner L., Williams-Stroud S., Hill A., Duncan P. and Thornton M. 2010. Beyond the dots in the box: Microseismicity-constrained fracture models for reservoir simulation. *The Leading Edge* **29**, 326–333.

Grechka V. and Tsvankin I. 2003. Feasibility of seismic characterisation of multiple fracture sets. *Geophysics* **68**, 1399–1407.

Hall S.A. and Kendall J.-M. 2000. Constraining the interpretation of AVOA for fracture characterisation. In: *Anisotropy 2000: Fractures, Converted Waves, and Case Studies* (eds L. Ikelle and A. Gangi), pp. 107–144. SEG.

Hall S.A., Kendall J.-M., Maddock J. and Fisher Q. 2008. Crack density tensor inversion for analysis of changes in rock frame architecture. *Geophysical Journal International* **173**, 577–592.

Holmes G.M., Crampin S. and Young R.P. 2000. Seismic anisotropy in granite at the Underground Research Laboratory, Manitoba. *Geophysical Prospecting* **48**, 415–435.

Horne S. and MacBeth C. 1994. Inversion for seismic anisotropy using genetic algorithms. *Geophysical Prospecting* **42**, 953–974.

Horne S., MacBeth C., Queen J., Rizer W. and Cox V. 1997. Fracture characterization from near offset VSP inversion. *Geophysical Prospecting* **45**, 141–164.

Hudson J.A. 1981. Wave speeds and attenuation of elastic waves in material containing cracks. *Geophysical Journal of the Royal Astronomical Society* **64**, 133–150.

Hudson J.A., Liu E. and Crampin S. 1996. The mechanical properties of materials with interconnected cracks and pores. *Geophysical Journal International* **124**, 105–112.

Keir D., Kendall J.-M., Ebinger C.J. and Stuart G.W. 2005. Variations in late syn-rift melt alignment inferred from shear-wave splitting in crustal earthquakes beneath the Ethiopian rift. *Geophysical Research Letters* **32**, L23308.

Kendall J.-M., Fisher Q.J., Covey Crump S., Maddock J., Carter A., Hall S.A. *et al*. 2007. Seismic anisotropy as an indicator of reservoir quality of siliclastic rocks. In: *Structurally Complex Reservoirs* (eds S. Jolley, D. Barr, J. Walsh and R. Knipe), pp. 123–136. Geological Society of London.

Kendall J.-M., Pilidou S., Keir D., Bastow I.D., Stuart G.W. and Ayele A. 2006. Mantle upwellings, melt migration and magma assisted rifting in Africa: Insights from seismic anisotropy. In: *Structure and Evolution of the Rift Systems within the Afar Volcanic Province, Northeast Africa* (eds G. Yirgu, C.J. Ebinger and P.K.H. Maguire), pp. 57–74. Geological Society of London.

Kendall J.-M., Stuart G.W., Ebinger C.J., Bastow I.D. and Keir D. 2005. Magma assisted rifting in Ethiopia. *Nature* **433**, 146–148.

Le Calvez J.H., Bennet L., Tanner K.V., Grant W.D., Nutt L., Jochen V. *et al*. 2005. Monitoring microseismic fracture development and production in aging fields. *The Leading Edge* **24**, 72–75.

Luo M., Takahashi I., Takanashi M. and Tamura Y. 2005. Improved fracture network mapping through reducing overburden influence. *The Leading Edge* **24**, 1094–1098.

Luo M., Takanashi M., Nakayama K. and Ezaka T. 2007. Physical modeling of overburden effects. *Geophysics* **72**, T37–T45.

Pointer T., Liu E. and Hudson J.A. 2000. Seismic wave propagation in cracked porous media. *Geophysical Journal International* **142**, 199–231.

Rial J.A., Elkibbi M. and Yang M. 2005. Shear-wave splitting as a tool for the characterization of geothermal fractured reservoirs: lessons learned. *Geothermics* **34**, 365–385.

Rümpker G., Tommasi A. and Kendall J.-M. 1999. Numerical simulations of depth-dependent anisotropy and frequency-dependent wave propagation effects. *Journal of Geophysical Research* **104**, 23141–23153.

Rutledge J.T., Phillips W.S. and Mayerhofer M.J. 2004. Faulting induced by forced fluid injection and fluid flow forced by faulting: An interpretation of hydraulic fracture microseismicity, Carthage Cotton Valley Gas Field, Texas. *Bulletin of the Seismological Society of America* **94**, 1817–1830.

Schoenberg M. and Sayers C.M. 1995. Seismic anisotropy of fractured rock. *Geophysics* **60**, 204–211.

Shuck E.L., Davis T.L. and Benson R.D. 1996. Multicomponent 3-D characterization of a coalbed methane reservoir. *Geophysics* **61**, 315–330.

Silver P.G. and Chan W.W.J. 1991. Shear-wave splitting and subcontinental mantle deformation. *Journal of Geophysical Research* **96**, 16429–16454.

Teanby N.A., Kendall J.-M., Jones R.H. and Barkved O. 2004a. Stress-induced temporal variations in seismic anisotropy observed in microseismic data. *Geophysical Journal International* **156**, 459–466.

Teanby N.A., Kendall J.-M. and Van Der Baan M. 2004b. Automation of shear-wave splitting measurements using cluster analysis. *Bulletin of the Seismological Society of America* **94**, 453–463.

Thomsen L. 1986. Weak elastic anisotropy. *Geophysics* **51**, 1954–1966.

Tod S.R. 2002. The effects of stress and fluid pressure on the anisotropy of interconnected cracks. *Geophysical Journal International* **149**, 149–156.

Valcke S.L.A., Casey M., Lloyd G.E., Kendall J.-M. and Fisher Q.J. 2006. Lattice preferred orientation and seismic anisotropy in sedimentary rocks. *Geophysical Journal International* **166**, 652–666.

Verdon J.P. 2010. *Microseismic monitoring and geomechanical modelling of CO_2 storage in subsurface reservoirs*. PhD thesis, University of Bristol.

Verdon J.P., Angus D.A., Kendall J.-M. and Hall S.A. 2008. The effects of microstructure and nonlinear stress on anisotropic seismic velocities. *Geophysics* **73**, D41–D51.

Verdon J.P., Kendall J.-M. and Wüstefeld A. 2009. Imaging fractures and sedimentary fabrics using shear wave splitting measurements made on passive seismic data. *Geophysical Journal International* **179**, 1245–1254.

Verdon J.P., Kendall J.-M. and Maxwell S.C. 2010a. A comparison of passive seismic monitoring of fracture stimulation due to water versus CO_2 injection. *Geophysics* **75**, MA1–MA7.

Verdon J.P., White D.J., Kendall J.-M., Angus D.A., Fisher Q. and Urbancic T. 2010b. Passive seismic monitoring of carbon dioxide storage at Weyburn. *The Leading Edge* **29**, 200–206.

White D. 2009. Monitoring CO_2 storage during EOR at the Weyburn-Midale field. *The Leading Edge* **28**, 838–842.

Winterstein D.F., De G.S. and Meadows M.A. 2001. Twelve years of vertical birefringence in nine-component VSP data. *Geophysics* **66**, 582–597.

Wookey J. 2010. Direct probabilistic inversion of shear-wave data for anisotropy. *Bulletin of the Seismological Society of America* (sub judice).

Wookey J. and Helffrich G.R. 2008. Inferences on inner-core shear-wave anisotropy and texture from an observation of PKJKP waves. *Nature* **454**, 873–876.

Wüstefeld A., Al-Harrasi O., Verdon J.P., Wookey J. and Kendall J.-M. 2010. A strategy for automated analysis of passive microseismic data to study seismic anisotropy and fracture characteristics. *Geophysical Prospecting* **58**, 755–773.